Osteoporosis

Figure removed due to copyright restrictions. See Figure 1: Vajjhala, S., A. M. Kraynik, et al. "A Cellular Solid Model for Modulus Reduction due to Resorption of Trabecular Bone." *Journal of Biomechanical Engineering* 122, no. 5 (2000): 511–15.

- As trabeculae thin - buckling easier $\quad \sigma^* \propto (\rho/\rho_s)^2$
- Once trabeculae begin to resorb, connectivity reduced, strength drops dramatically
- Modeling:
  - Can't use unit cell or dimensional analysis (need to model local effects)
  - Finite element modeling
  - Initially: $\left.\begin{array}{l} -\ 2D \text{ Voronoi honeycombs} \\ -\ 2D \text{ representation of vertebral bone} \end{array}\right\}$ Matt Silva
    - $3D$ Voronoi foam — Surekha Vajjbala

Voronoi honeycomb

- Random seed points, draw perpendicular bisectors
- Use a minimum separation distance to get cells of approximately uniform size
- FE analysis — each trabecula a beam element
- First calculated elastic moduli
  - FEA results close to analytical model for random (isotropic) honeycomb (40 models, all same ρ^*/ρ_s, about 25x25 cells in each)
  - Modulus is average of stiffness over entire material

Modelling: 2D Voronoi

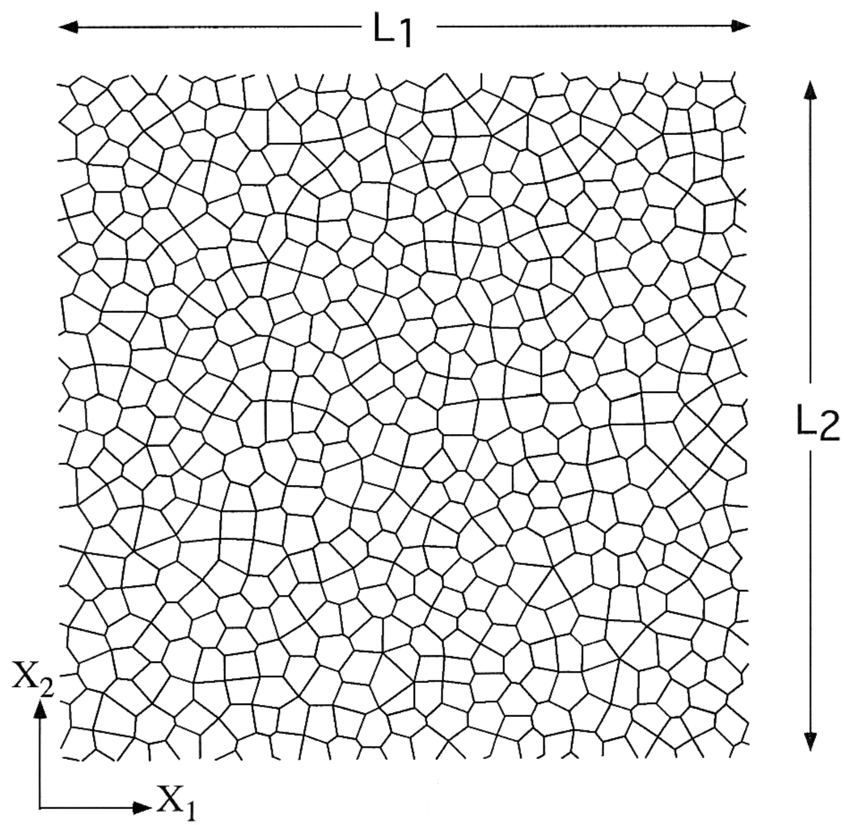

Silva et al, 1995

2D Voronoi

E^*/E_s	FEA	$y=0.56x^{2.43}$
E^*/E_s	Equation (1a)	$y=0.63x^{2.54}$
G^*/E_s	FEA	$y=0.18x^{2.53}$
G^*/E_s	Equation (3d)	$y=0.20x^{2.68}$
ν^*	FEA	$y= -1.20x^{1.38} + 1.0$
ν^*	Equation (1b)	$y= -1.30x^{1.55} + 1.0$

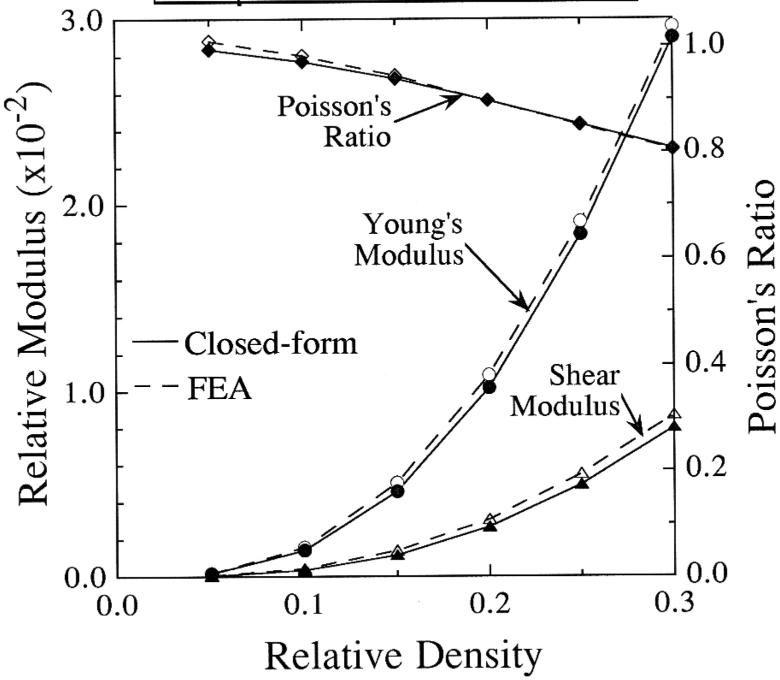

Silva et al, 1995

- Next, calculated compressive strength of Voroni honeycombs
- Each cell wall 1-3 beam elements
- Model non-linear elasticity and failure behavior
- 15x15 cells in model (random seeds $\approx$ isotropic)
- Cell wall assumed to be elastic – perfectly plastic $\sigma_{\text{ys}}/E_s = 0.01 \quad \upsilon_s = 0.3$
- For this value of σ_{ys}/E_s, transition between elastic buckling and plastic collapse stress at $\rho^*/\rho_s = 0.035$ in regular hexagonal honeycomb
- Calculated compressive strength of honeycombs with $\rho^*/\rho_s = 0.015,\ 0.035,\ 0.05,\ 0.15$
- Generated 5 different Voronoi honeycombs at each ρ^*/ρ_s
- Compressive $\sigma - \epsilon$ behavior:

$\rho^*/\rho_s \geq 0.05$	-strain softening, permanent deformation on unloading
	-plastic hinge formation, cell collapse in narrow localized bands
$\rho^*/\rho_s < 0.035$	-non-linear elastic deformation - recoverable
Strength:	0.6 to 0.8 of $\sigma^*_{\text{periodic}}$

2D Voronoi

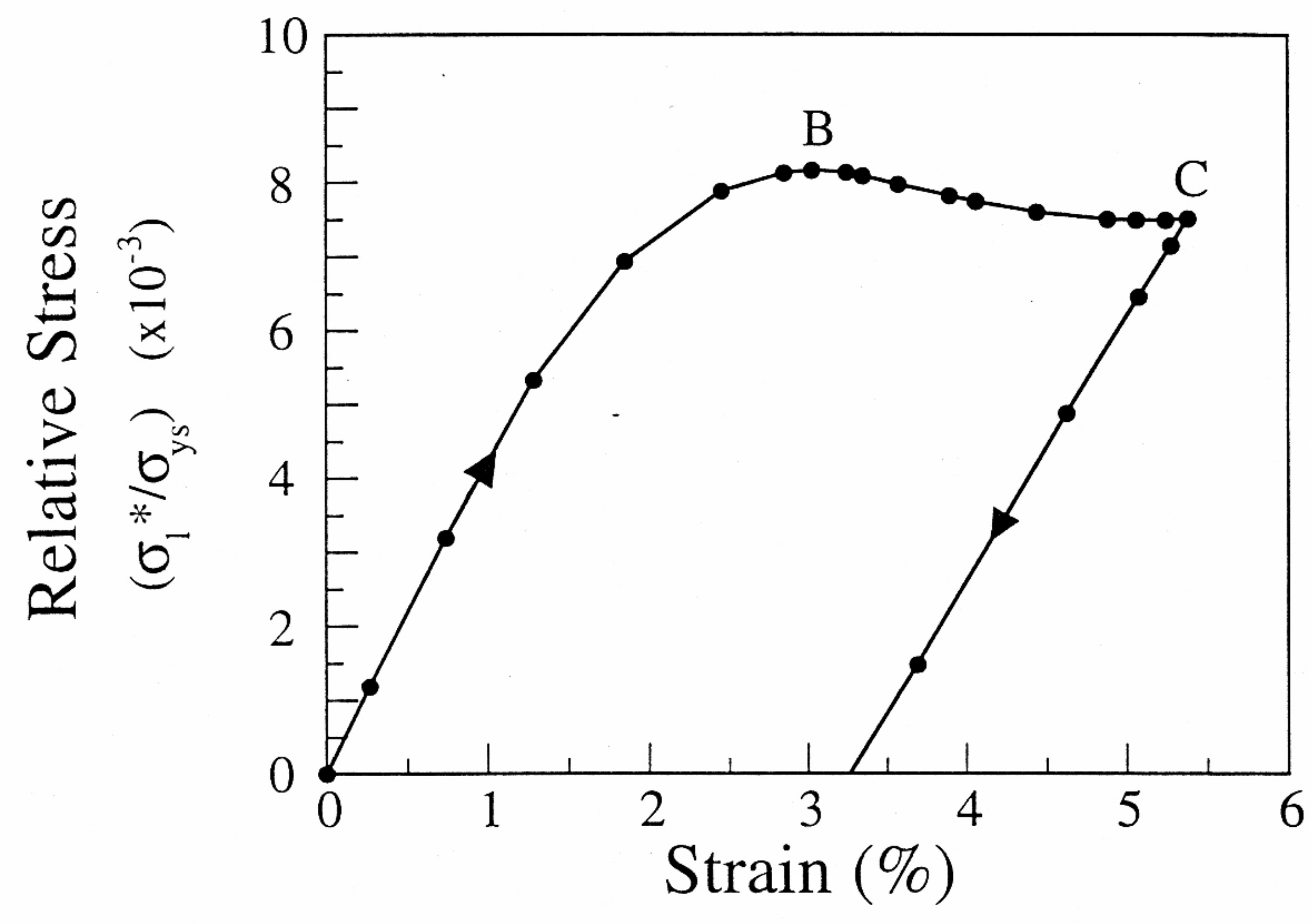

Relative density = 15% Plastic failure

Silva et al, 1997

Source: Silva, M. J., and L. J. Gibson. "The Effects of Non-periodic Microstructure and Defects on the Compressive Strength of Two-dimensional Cellular Solids." *International Journal of Mechanical Sciences* 39 (1997b): 549-63. Courtesy of Elsevier. Used with permission.

2D Voronoi

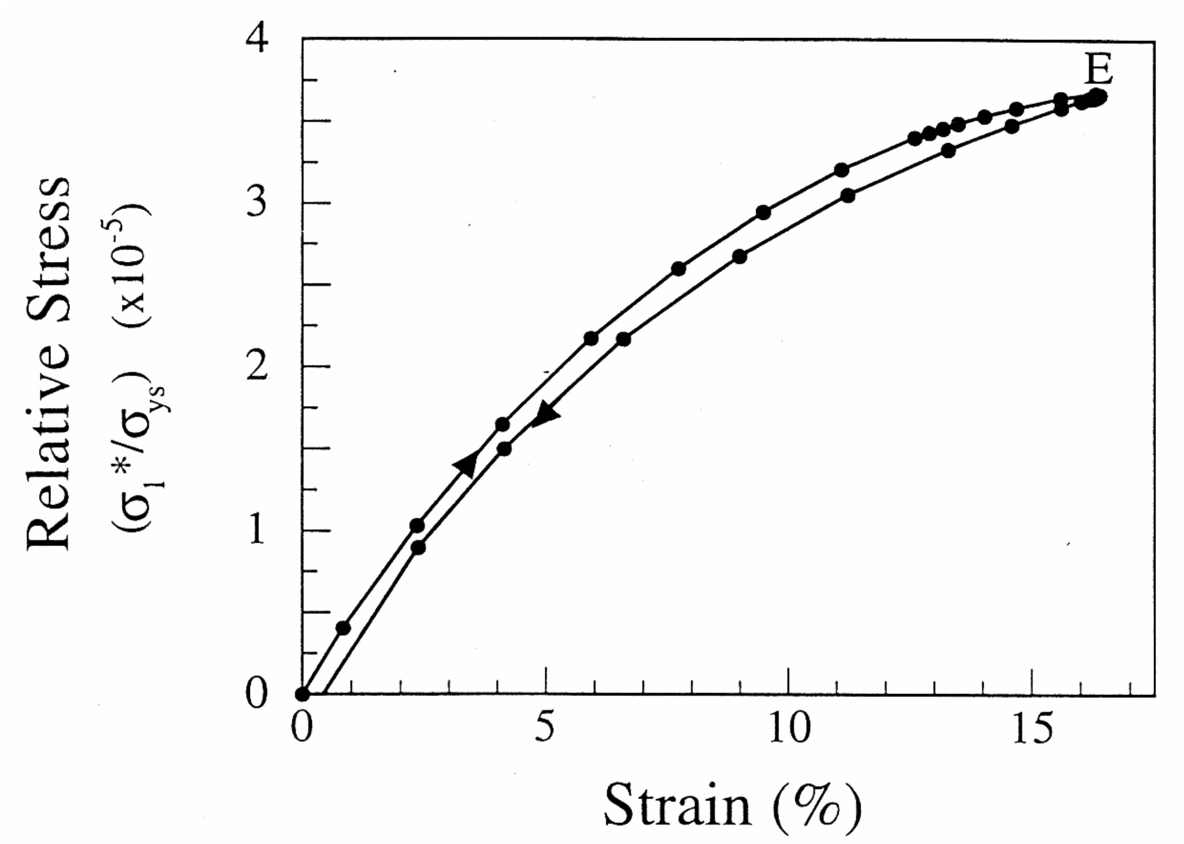

Relative density 1.5%; elastic buckling failure

Silva et al, 1997

Source: Silva, M. J., and L. J. Gibson. "The Effects of Non-periodic Microstructure and Defects on the Compressive Strength of Two-dimensional Cellular Solids." *International Journal of Mechanical Sciences* 39 (1997b): 549-63. Courtesy of Elsevier. Used with permission.

2D Voronoi

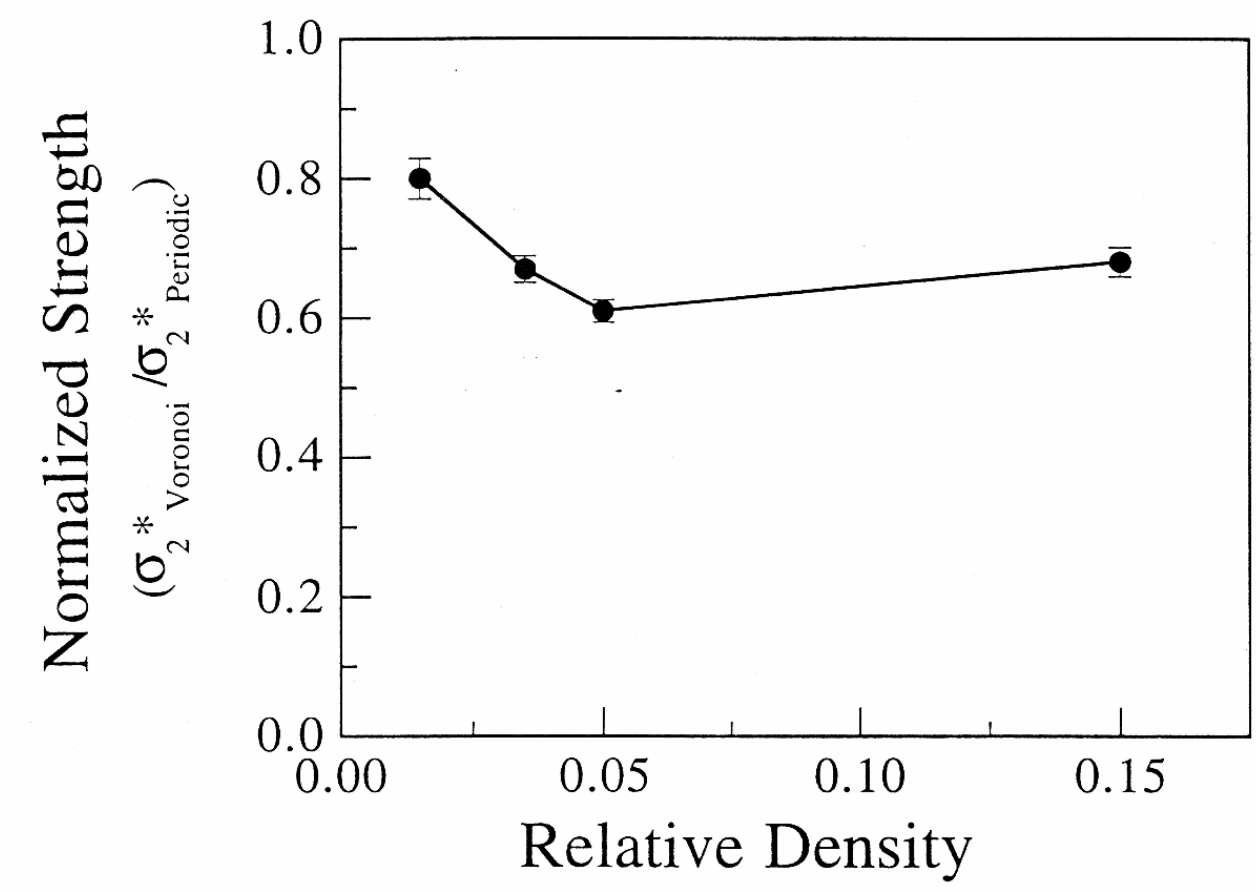

Silva et al, 1997

Source: Silva, M. J., and L. J. Gibson. "The Effects of Non-periodic Microstructure and Defects on the Compressive Strength of Two-dimensional Cellular Solids." *International Journal of Mechanical Sciences* 39 (1997b): 549-63. Courtesy of Elsevier. Used with permission.

- Max. normal strains at nodes in honeycombs (linear elastic).
  - Voronoi honeycombs — normal distribution
  - Regular hexagonal honeycombs — dashed lines on plot
  - Normal strain in vertical cell walls in regular hexagonal honey combs — mean normal strain in Voronoi
  - Oblique walls — bending — larger strains
  - Voronoi honeycomb 5% of strain outside of range of strain in regular hexagonal honeycomb
  - Decrease in strength associated with broader range of strains in Voronoi honeycombs
  - Minimum strength at $\rho^*/\rho_s = 0.05$
    — Interaction between elastic buckling and plastic yield

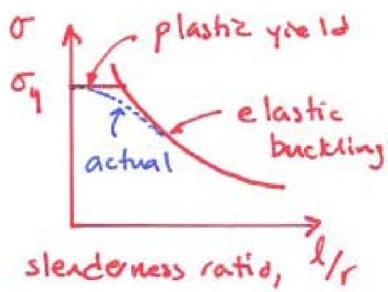

$$\sigma_{cr} = \frac{\pi^2 EI}{l^2} = \frac{\pi^2\, E\, \pi\, r^4}{4\, l^2\, \pi\, r^2} = \frac{\pi^2}{4} E \left(\frac{r}{l}\right)^2$$

2D Voronoi

Figure removed due to copyright restrictions. See Figure 5; Silva, M. J., and L. J. Gibson. "The Effects of Non-periodic Microstructure and Defects on the Compressive Strength of Two-dimensional Cellular Solids." *International Journal Mechanical Sciences* 39, no. 5 (1997): 549-63.

Silva et al, 1997

Voronoi honeycombs - defects

- Randomly removed cell walls in both Voronoi and regular honeycombs
- Analyzed both by FEA
- Dramatic decrease in modulus and strength, compared with equivalent reduction in density by thinning of cell walls
- $\rho^*/\rho_s = 0.15$ failure by yielding
- $\rho^*/\rho_s = 0.015$ failure by elastic buckling
- Modulus and strength reduction similar for Voronoi and regular hexagonal honeycombs
- Percolation threshold for $2D$ network hexagonal cells $\Rightarrow$ 35% struts removed

Vertebral trabecular bone - 2D model

- Model adapted to reflect trabeculae more aligned in vertical and horizontal directions
- Perturbed a square array of struts to get similar orientation and struts as in bone
- Looked at reduction in number and thickness of longitudinal and transverse struts (independently)

2D Voronoi

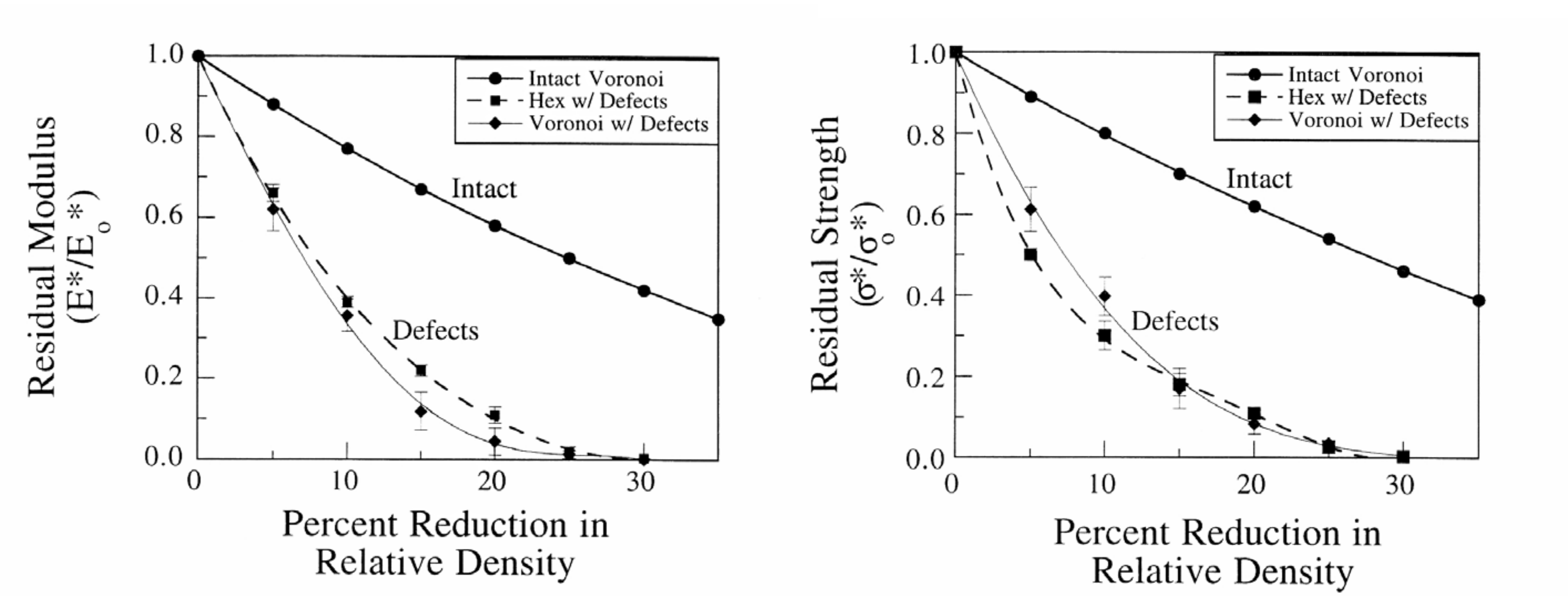

Source: Silva, M. J., and L. J. Gibson. "The Effects of Non-periodic Microstructure and Defects on the Compressive Strength of Two-dimensional Cellular Solids." *International Journal of Mechanical Sciences* 39 (1997b): 549-63. Courtesy of Elsevier. Used with permission.

Silva et al, 1997

2D Voronoi

Figure removed due to copyright restrictions. See Figure 2: Vajjhala, S., A. M. Kraynik, et al. "A Cellular Solid Model for Modulus Reduction due to Resorption of Trabecular Bone." *Journal of Biomechanical Engineering* 122, no. 5 (2000): 511–15.

Vajjhala et al, 2000

Vertebral Trabecular Bone

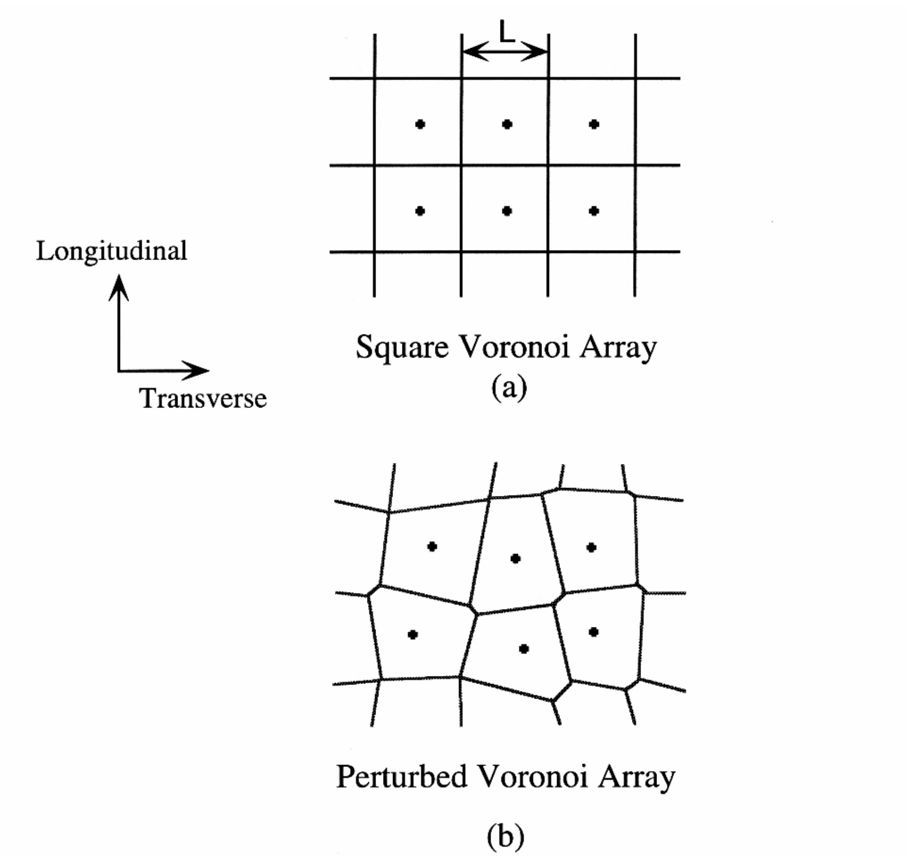

Source: Silva, M. J., and L. J. Gibson. "Modelling the Mechancial Behavior of Vertebral Trabecular Bone: Effects of Age-related Changes in Microstructure." *Bone* 21 (1997a): 191-99. Courtesy of Elsevier. Used with permission.

Silva et al, 1997

Vertebral Trabecular Bone

Figure removed due to copyright restrictions. See Figure 3: Silva, M. J., and L. J. Gibson. "Modelling the Mechancial Behavior of Vertebral Trabecular Bone: Effects of Age-related Changes in Microstructure." *Bone* 21 (1997): 191-99.

Silva et al, 1997

Vertebral Trabecular Bone

Figure removed due to copyright restrictions. See Figure 4: Silva, M. J., and L. J. Gibson. "Modelling the Mechancial Behavior of Vertebral Trabecular Bone: Effects of Age-related Changes in Microstructure." *Bone* 21 (1997): 191-99.

Silva et al, 1997

Vertebral Trabecular Bone

Figure removed due to copyright restrictions. See Figure 5: Silva, M. J., and L. J. Gibson. "Modelling the Mechancial Behavior of Vertebral Trabecular Bone: Effects of Age-related Changes in Microstructure." *Bone* 21 (1997): 191-99.

Silva et al, 1997

Vertebral Trabecular Bone

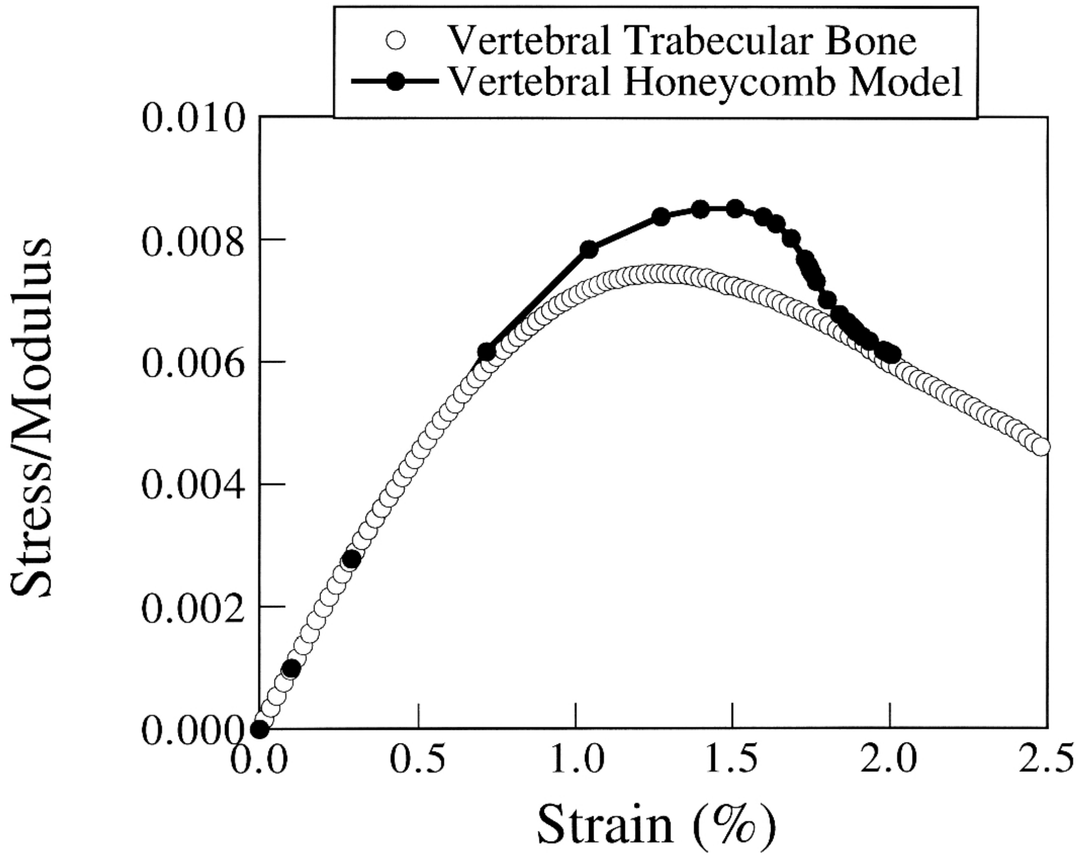

Silva et al, 1997

Source: Silva, M. J., and L. J. Gibson. "Modelling the Mechancial Behavior of Vertebral Trabecular Bone: Effects of Age-related Changes in Microstructure." *Bone* 21 (1997a): 191-99. Courtesy of Elsevier. Used with permission.

Vertebral Trabecular Bone

Silva et al, 1997

Vertebral Trabecular Bone

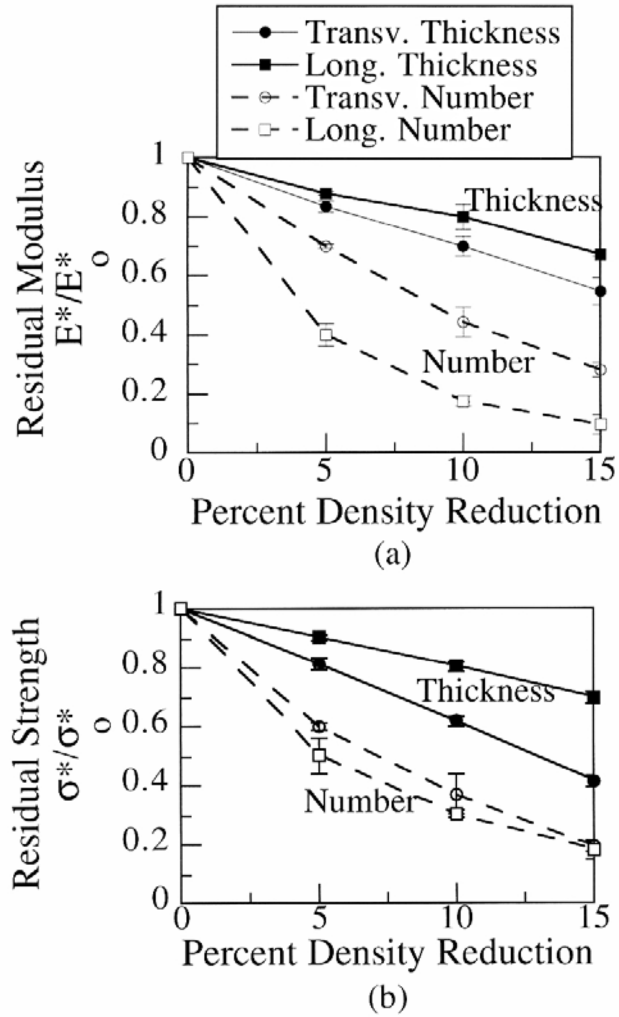

Silva et al, 1997

Source: Silva, M. J., and L. J. Gibson. "Modelling the Mechancial Behavior of Vertebral Trabecular Bone: Effects of Age-related Changes in Microstructure." *Bone* 21 (1997a): 191-99. Courtesy of Elsevier. Used with permission.

3D Voronoi Model

- Same analysis, now with 3D Voronoi model
- Periodic 3x3x3 cells, $\rho^*/\rho_s = 0.1$
- Used beam elements, FEA, linear elastic only
- Percolation threshold $\sim 50\%$ struts removed
- Comparison of 2D and 3D results for modulus: in 3D, modulus reduction more gradual than in 2D
- Also for 2D and 3D — modulus reduction similar for regular and Voronoi structures

3D Voronoi Model

Figure removed due to copyright restrictions. See Figure 7: Vajjhala, S., A. M. Kraynik, et al. "A Cellular Solid Model for Modulus Reduction due to Resorption of Trabecular Bone." *Journal of Biomechanical Engineering* 122, no. 5 (2000): 511–15.

Vajjhala et al, 2000

3D Voronoi Model

Figure removed due to copyright restrictions. See Figure 7: Vajjhala, S., A. M. Kraynik, et al. "A Cellular Solid Model for Modulus Reduction due to Resorption of Trabecular Bone." *Journal of Biomechanical Engineering* 122, no. 5 (2000): 511–15.

Vajjhala et al, 2000

Metal foams as bone substitute materials

- Metals used in orthopedic implants (e.g. hip, knee)
- Co-Ci, Ti, Ta, stainless steel alloys
- Biocompatible, corrosion resistant
- But moduli of metals are greater than modulus of bone
  e.g. $E_{\mathrm{Ti}} = 110$ GPa, $E_{\mathrm{cortical}} = 18$ GPa, $E_{\mathrm{trab.bone}} = 0.01 - 2$ GPa
- Stress shielding can lead to bone resorption
- To improve mechanical interaction between implant and bone:
  - porous sintered metal beads used to coat implants - promote bone ingrowth
  - also, wire mesh coatings have been developed, primarily for flat implant surfaces
  - recently, interest in using metal foams as coatings
  - longer term, interest in using in replacement vertebral bodies
- Variety of processes for making metal foam implant coatings

Metal Foams: Microstructure

Ta, replicating PU foam with CVD

Ti, replication of PU foam by slurry infiltration and sintering

Ti, fugitive phase

Ti, foaming agent

Images removed due to copyright restrictions. See Figure 8.1: Gibson, L. J., M. Ashby, and B. A. Harley. *Cellular Materials in Nature and Medicine*. Cambridge University Press, 2010. http://books.google.com/books?id=AKxiS4AKpyEC&pg=PA228

Ti, expansion of Ar gas

Ti, freeze-casting (freeze-drying)

Ti, selective laser sintering

Ni-Ti, high temperature synthesis (powders mixed, pressed and ignited by, for example, tungsten coil heated by electrical current)

Image sources given in Cellular Materials in Nature and Medicine

Processing

(a) Replicate open cell polyurethane foam

- Pyrolize PU foam $\rightarrow$ 2% dense vitreous carbon
- Coat with Ta by CVD $\Rightarrow$ struts 99% Ta, 1% C
- Cell size $400 - 600\ \mu$m; coating thickness $40 - 60\ \mu$m, $\rho^*/\rho_s = 0.15 - 0.25$
- "Trabecular metal" (Zimmer) trade name
- Ta forms surface oxide Ta_2O_5 — does not bond to bone
- But, if treat with dilute NaOH, then heat to 300°C and cool, then submerge in simulated body fluid (ion concentration matches human blood plasma)
  $\Rightarrow$ get apatite coating on foam struts, which bonds to bone

(b) Infiltrate slurry of titanium hydride into open cell foam

- Heat-treat to decompose TiH_2
- Sinter remaining Ti (also removes initial foam)

(c) Fugitive phase methods

- Mix Ti powder and fugitive phase powder
- Heat to T_1 ($\sim 200^\circ\ C$) to decompose filler, then to T_2 ($1200^\circ\ C$) to sinter Ti powder

Metal Foams: Processing

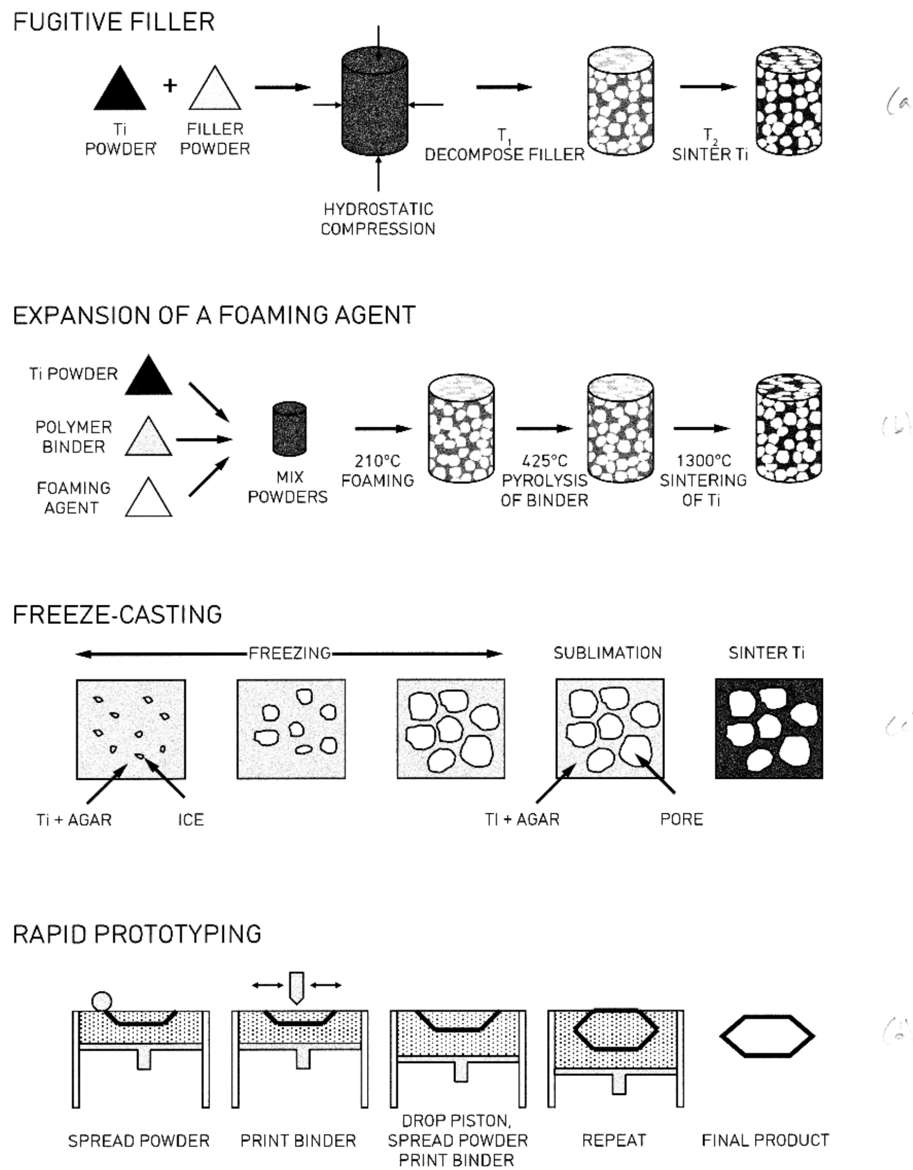

Foaming agent evolves gas at temperature at which polymer is liquid

Gibson, L. J., M. Ashby, et al. *Cellular Materials in Nature and Medicine*. Cambridge University Press, © 2010. Figures courtesy of Lorna Gibson and Cambridge University Press.

Processes

(d) Expansion of foaming agent

(e) Freeze casting (freeze dying)

(f) Rapid prototyping (3D Printing, selective laser sintering)

$\sigma - \epsilon$ curves - similar to other foams

Data for E^*, σ_c^*

Ti Foam: Stress-strain

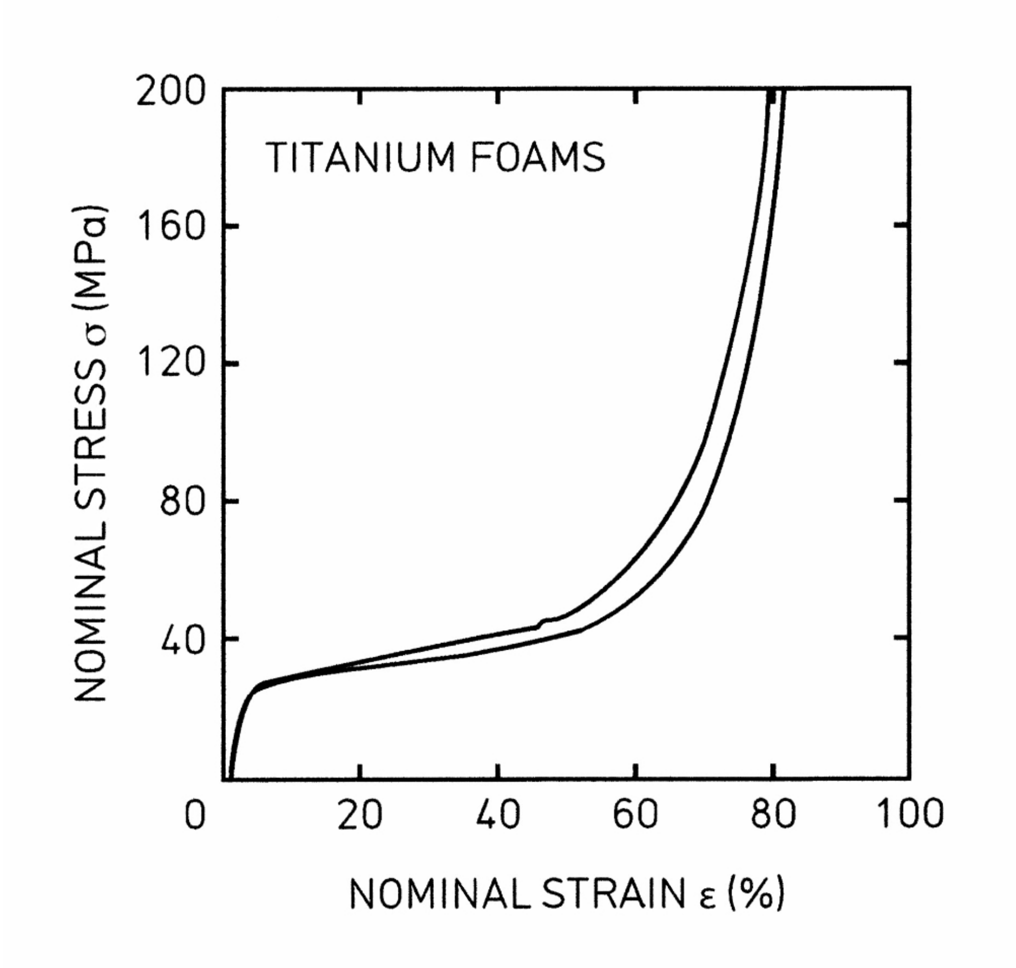

Source: Wen, C. E., M. Mabuchi, et al. "Processing of Biocompatible Porous Ti and Mg."
Scripta Materialia 45 (2001): 1147-53. Courtesy of Elsevier. Used with permission.

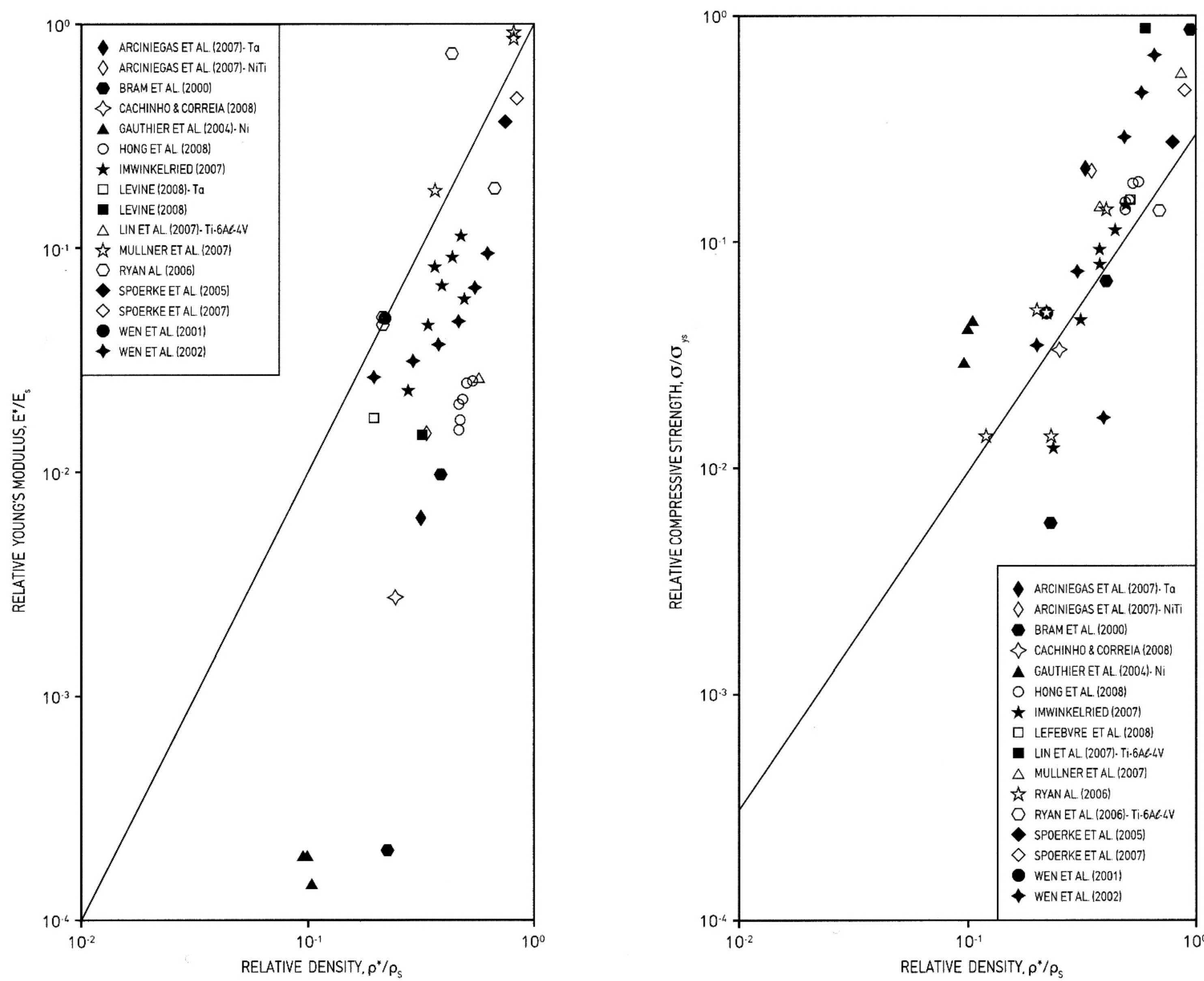

Gibson, L. J., M. Ashby, et al. *Cellular Materials in Nature and Medicine*. Cambridge University Press, © 2010. Figures courtesy of Lorna Gibson and Cambridge University Press.

Bone in Evolutionary Studies

Bone structure in evolutionary studies

- Phylogenetic chart — big picture — structural biomaterials (mineralized)
- Sponges — first multi-celled animal
  - calcarea: $CaCO_3$ spicules (needles)
  - hexactinellida: SiO_2 — "glass sponges"
  - demospongiae: most sponges — some have SiO_2 spicules
    — spongin (type of collagen)
- Cnidarians - e.g. corals, jellyfish
  - Corals $CaCO_3$
- Mollusca — bivalves, snails, octopus
  - if mineralized $CaCO_3$
- Arthropods e.g. hexapoda (insects), arachnide (spiders), crustaceans (shrimp, lobster)
  - Exoskeleton of insects and spiders: chitin
  - Crustaceans: chitin may be mineralized with $CaCO_3$

Vertebrates

- Cyclostomata
  - jawless fish — lampreys hagfish
  - no vertebra — notochord
  - no bone
- Chondrichthye
  - sharks, rays, skates
  - cartilagenous skeleton — some mineralization, but not true bone
- Actinopterygii
  - ray-finned fish
  - true bone
  - 450 million years ago

Bone structure and loading

- Bone grows in response to loading
- Bone structure reflects mechanical loading and function; e.g. quadruped vs. biped
- Evolutionary studies have looked at trabecular bone architecture and density

METAZOA

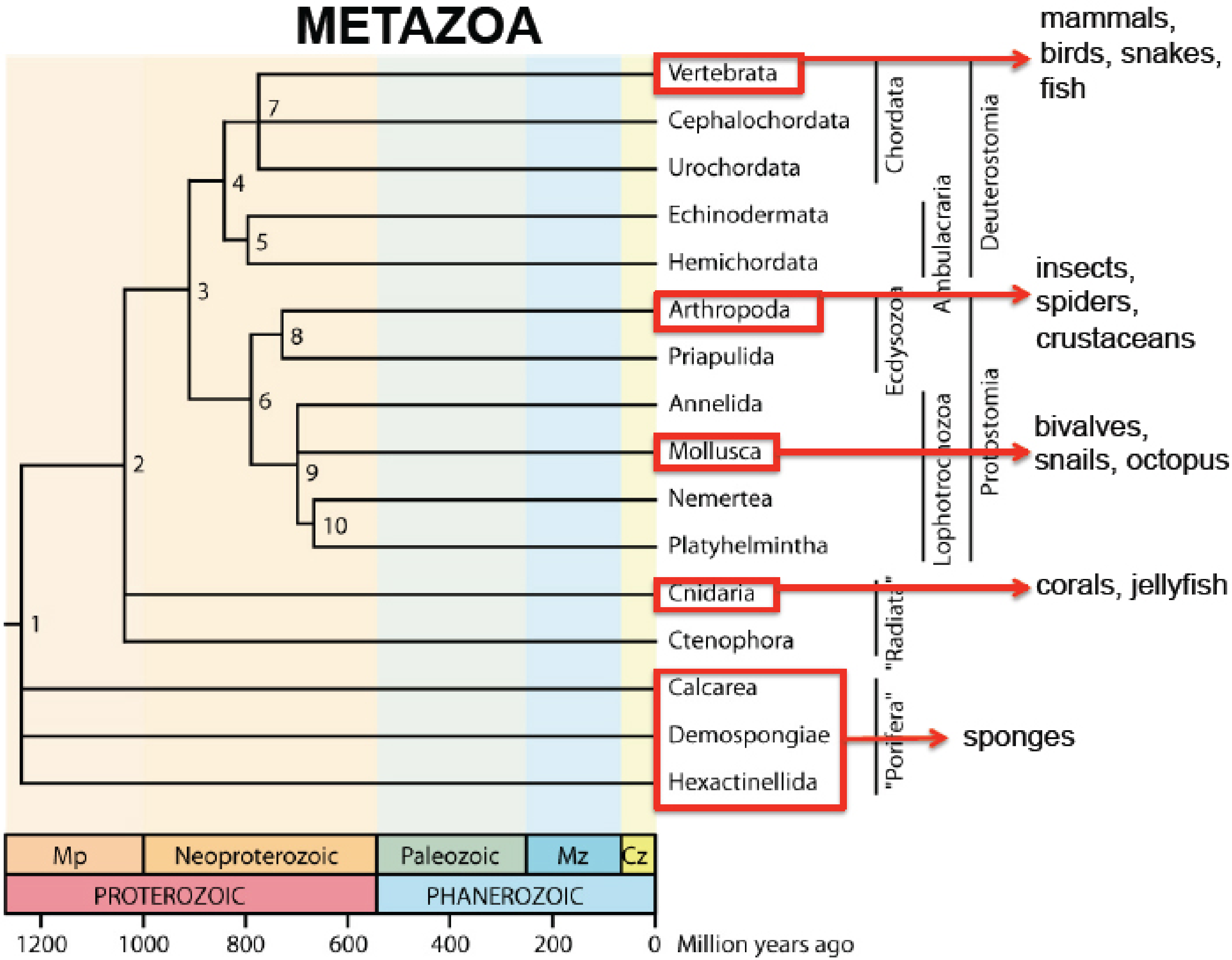

Fig. 2 A timetree of metazoan phyla. Divergence times are shown in Table 1. *Abbreviations*: Cz (Cenozoic), Mp (Mesoproterozoic), and Mz (Mesozoic).

Hedges and Kumar, 2009

Venus Flower Basket
(*Euplectella aspergillum*)

- Hierarchical structure
- Remarkably stiff, tough
- Joanna Aizenberg (Harvard)
- Aizenberg et al (2004) Biological glass fibers: correlation between optical and structural properties. PNAS

VERTEBRATA

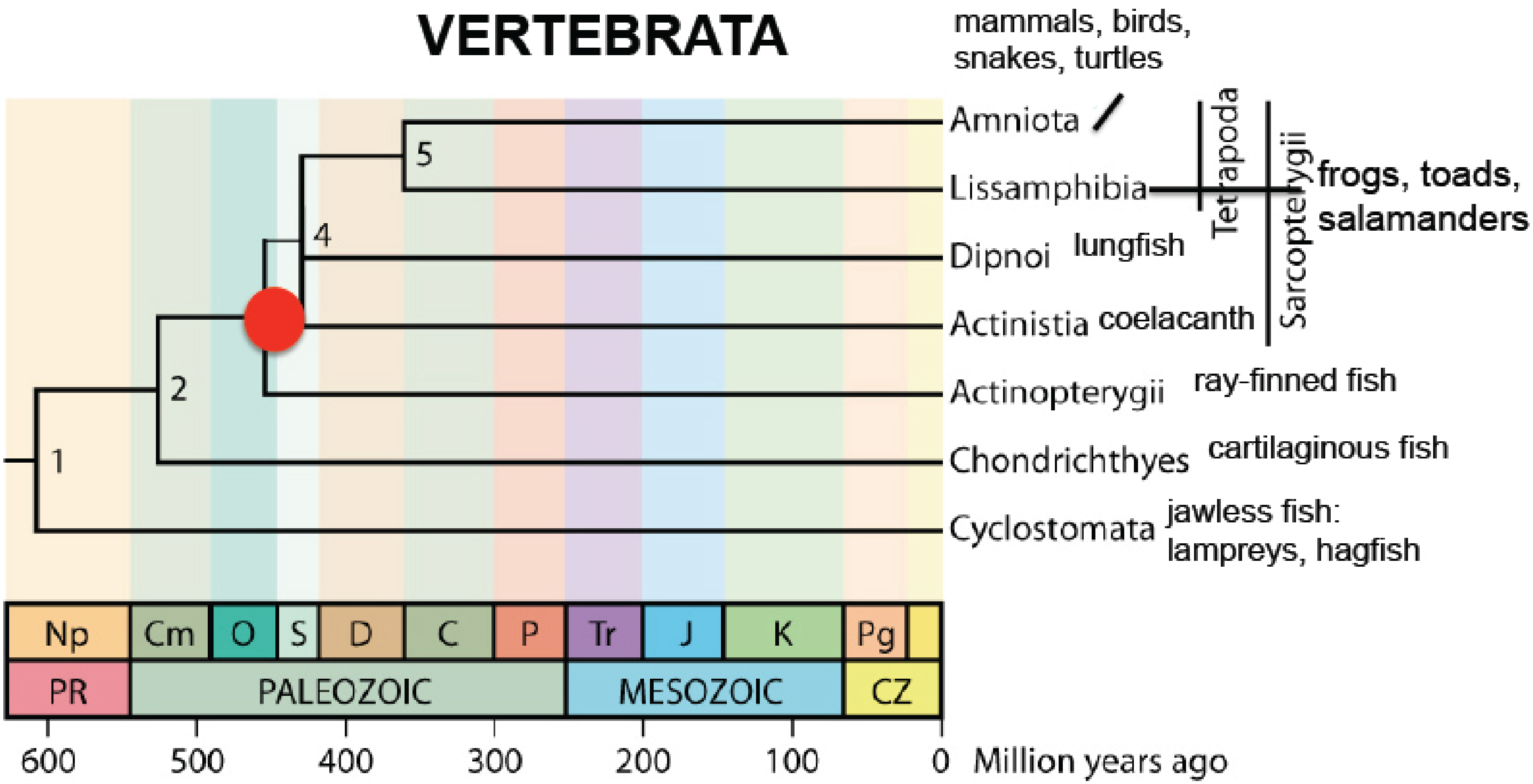

Fig. 2 A timetree of vertebrates. Times of divergence are averages of estimates from different studies listed in Table 1. *Abbreviations*: C (Carboniferous), Cm (Cambrian), CZ (Cenozoic), D (Devonian), J (Jurassic), K (Cretaceous), Np (Neoproterozoic), O (Ordovician), P (Permian), Pg (Paleogene), PR (Proterozoic), S (Silurian), and Tr (Triassic).

Common ancestor of all boned vertebrates roughly 450 MYA

(Hagfish video)

Hedges and Kumar, 2009

Trabecular bone studies in human evolution

Oreopithecus bambolii (Rook et al, 1999)

- 7-9 Million years ago, late Miocene hominid, found in Italy
- Quadruped or biped?
- Compared trabecular architecture in ilium in apes, o. bambolii, humans
- Only had two fragments of ilium — left and right
- Took radiographs of both and digitally reconstructed a single ilium

Comparisons

(a) Posterosuperior margin — marginal handles thicker than apes

(b) Anteriosuperior margin — iib bundle relatively structured compared to apes

(c) Anterioinferior margin — well-developed a-i spine not seen in apes

(d) Supra acetabular area — high density region

- Collectively, observations suggest O. bambolii trab. architecture in ilium more similar to humans than apes
- Suggests habitual bipedal locomotion (humans — obligatory bipeds)

Oreopithecus bambolii: Ilium

Rook et al. (1999)

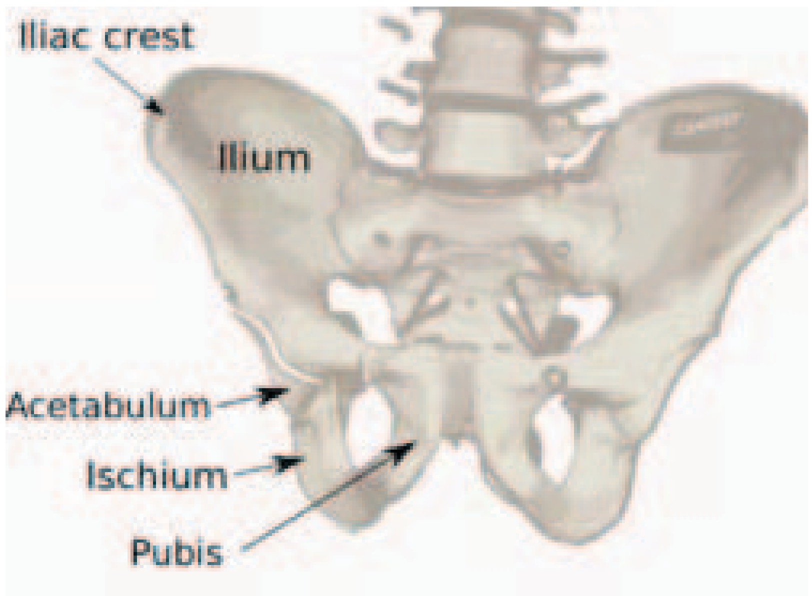

http://en.wikipedia.org/wiki/Iliac_crest

Trabecular architecture: Ilium

Figure removed due to copyright restrictions. See Figure 1: Rook L., et al. "Oreopithecus was a Bipedal Ape after All." *Proceedings of the Natural Academy of Sciences* 96 (1999): 8795-99.

Digitally reconstructed ilium

Comparison of trabecular architecture

Figure removed due to copyright restrictions. See Figure 3: Rook L., et al. "Oreopithecus was a Bipedal Ape after All." *Proceedings of the Natural Academy of Sciences* 96 (1999): 8795-99.